

Received: 2015.06.26
Accepted: 2015.07.01
Published: 2015.10.29

Subject-Specific Fully-Coupled and One-Way Fluid-Structure Interaction Models for Modeling of Carotid Atherosclerotic Plaques in Humans

Authors' Contribution:
Study Design A
Data Collection B
Statistical Analysis C
Data Interpretation D
Manuscript Preparation E
Literature Search F
Funds Collection G

BCDEF **Xiaojuan Tao**
ABCDEFG **Peiyi Gao**
BCDF **Lina Jing**
CDF **Yan Lin**
BCF **Binbin Sui**

Department of Radiology, Beijing Tian Tan Hospital, Capital Medical University, Beijing, P.R. China

Corresponding Author: Peiyi Gao, e-mail: cjr.gaopeiyyi@vip.163.com

Source of support: This work was supported by the National Key Project of Scientific and Technical Supporting Programs Funded by Ministry of Science & Technology of China During the 11th Five-year Plan (No. 2007BAI05B07), the Beijing Natural Science Foundation (No. 7002011) and the Capital Medical Development and Research Foundation, China (No. 2005-2026)

Background: Hemodynamics play an important role in the development and progression of carotid atherosclerosis, and may be important in the assessment of plaque vulnerability. The aim of this study was to develop a system to assess the hemodynamics of carotid atherosclerotic plaques using subject-specific fluid-structure interaction (FSI) models based on magnetic resonance imaging (MRI).

Material/Methods: Models of carotid bifurcations (n=86 with plaques from 52 patients, n=14 normal carotids from 12 participants) were obtained at the Department of Radiology, Beijing Tian Tan Hospital between 2010 and 2013. The maximum von Mises stress, minimum pressure, and flow velocity values were assessed at the most stenotic site in patients, or at the carotid bifurcations in healthy volunteers. Results of one-way FSI were compared with fully-coupled FSI for the plaques of 19 randomly selected models.

Results: The maximum von Mises stress and the minimum pressure and velocity were significantly increased in the stenosis group compared with controls based on one-way FSI (all $P < 0.05$). The maximum von Mises stress and the minimum pressure were significantly higher and the velocity was significantly lower based on fully coupled FSI compared with on-way FSI (all $P < 0.05$). Although there were differences in numerical values, both methods were equivalent. The maximum von Mises stress of vulnerable plaques was significantly higher than stable plaques ($P < 0.001$). The maximum von Mises stress of the group with fibrous cap defect was significantly higher than the group without fibrous cap defect ($P = 0.001$).

Conclusions: The hemodynamics of atherosclerotic plaques can be assessed noninvasively using subject-specific models of FSI based on MRI.

MeSH Keywords: **Atherosclerosis • Carotid Arteries • Carotid Artery Diseases**

Full-text PDF: <http://www.medscimonit.com/abstract/index/idArt/895137>

 3694

 2

 3

 36



Background

Carotid artery stenosis (CAD) is the narrowing of the carotid artery lumen; it is commonly caused by atherosclerosis and leads to increased risk of transient ischemic attack and stroke [1–6]. CAD mostly affects men (male to female ratio of 2: 1), and is more common in patients >60 years old, in patients with coronary and/or peripheral atherosclerosis, in patients with diabetes, hypertension and/or dyslipidemia, and in patients who smoke [3,7]. In the United States, the estimated prevalence of CAD is 2–9% in the general population, 5–9% in people >65 years old, 11–26% in patients with coronary artery disease, and 11–49% in patients with peripheral atherosclerosis [7]. CAD prevalence even reached 58% in the North Manhattan Study [8].

The finding that atherosclerotic plaques tend to be located near an arterial bifurcation or bend has led to the wide acceptance of the concept that hemodynamic forces such as stress, pressure and velocity play important roles in the development and progression of atherosclerosis [9–11]. Nevertheless, despite many studies on the subject, a detailed understanding of the local hemodynamic environment is lacking, mainly because of the difficulties in measuring hemodynamic variables *in vivo*, as well as the wide inter-individual variations in vascular morphology.

In recent years, fluid-structure interaction (FSI) analysis has emerged as a tool that combines blood-flow simulation using computational fluid dynamics modeling with finite element analysis of the corresponding stress and pressure levels in the surrounding tissues [12–16]. In addition, due to the increased resolution and quality of MRI, it is now possible to distinctly, morphologically and structurally characterize atherosclerotic plaques *in vivo* to construct a subject-specific model of the carotid artery. However, this approach is in its infancy and further study is necessary before using this tool in the clinical setting. In addition, it is necessary to determine the parameters for abnormal carotid hemodynamics using this approach.

Therefore, the aim of the present study was to develop a platform to assess the abnormal hemodynamics of carotid atherosclerotic plaques using the subject-specific FSI model based on MRI. This MRI-based FSI model may enable the noninvasive assessment of the local hemodynamic parameters of atherosclerotic plaques *in vivo*, which could be used for the prevention and management of CAD.

Material and Methods

Subjects

High-resolution carotid MRI scans were obtained from 52 patients with carotid artery atherosclerosis and 12 healthy

participants without carotid artery atherosclerosis at the Department of Radiology, Beijing Tian Tan Hospital, Capital Medical University between 2010 and 2013. For patients, inclusion criteria were: 1) newly diagnosed with bilateral or unilateral carotid stenosis by ultrasound; 2) blood flow was still present; 3) received no treatment; and 4) with high image quality. Healthy participants underwent MRI for any reason and were without carotid artery atherosclerosis on MRI and with high image quality. Patients and controls were excluded if: 1) they received any drug treatment affecting atherosclerosis; or 2) they had any contraindication to MRI.

The study protocol was approved by the ethics committee of the Beijing Tian Tan Hospital. Individual consent was waived by the committee since images were used from patients who underwent MRI for a medical reason and because no additional testing was performed.

Study design

All MRI scans were retrospectively analyzed. Eighty-six diseased carotid arteries were examined. Fourteen normal carotid bifurcations from 12 controls were used as controls; not all bifurcations were used in controls because of shape asymmetry in some cases, and only one side was then used. Hemodynamics parameters were determined from the scans, and compared between the two groups.

Carotid high-resolution MRI

MRI was performed using a 3.0T MRI scanner (Trio-Tim; Siemens, Erlangen, Germany) at a maximum slew rate of 200 mT/m/ms and a maximum gradient strength of 45 mT/m. A four-element carotid surface coil (custom-made; Siemens Mindit, Shenzhen, China) was used to obtain images at a high signal-to-noise ratio.

The common carotid artery (CCA), the internal carotid artery (ICA) and the external carotid artery (ECA) were scanned in sequence. The protocol included four sequences in the axial plane: 1) time-of-flight (TOF) MRI: repetition time (TR) 21 ms, echo time (TE) 3.84 ms, flip angle 25°; 2) T2-weighted (T2W) MRI using turbo spin echo (TSE), TR 3000 ms, TE 65 ms; 3) proton density-weighted (PDW) MRI using TSE, TR 3000 ms, TE 13 ms; and 4) T1-weighted (T1W) MRI using black-blood (double-inversion recovery) 2-D TSE, cardiac-gated, TR 750 ms, TE 12 ms. For all sequences, the field-of-view was 14 cm; the matrix size was 320×240; the slice thickness was 2 mm (1 mm for TOF); and there were two signal means (1 for TOF). The in-plane resolution was 0.4×0.4 mm for TOF, PDW and T1W MRI or 0.5×0.5 mm for T2W MRI. Fat suppression was used to reduce signals from subcutaneous fatty tissue in the T2W, PDW, and T1W images. A validated protocol consisting of TOF,

T2W, PDW and T1W images of different signal intensities was used to identify the plaque components and the normal vessel walls, as previously described [17,18]. Plaque morphology was independently assessed by two mid-level observers (Tao XJ and Jing LN) with experience in assessment of carotid artery plaques; disagreements were solved by discussion. The carotid atherosclerotic plaques were classified according to the American Heart Association (AHA) classification and to MRI characteristics [19]. Patients with CAD were divided into the stable plaque group (AHA classification I-III) and the vulnerable plaque group (AHA classification IV-VIII). According to the status of the fibrous cap, the vulnerable plaque group was subdivided into the group without fibrous cap defect and the group with fibrous cap defect. Fibrous cap defects appear as rupture and ulceration, showing a low-signal band discontinuity on TOF MRI.

The blood flow velocity was calculated as the measured mean blood flow velocities at the CCA in the transverse plane perpendicular to the vessel and 2 cm below the apex of the carotid bifurcation, as measured using a cine phase-contrast MRI pulse sequence (MRI-PC). Retrospective peripheral gating (ECG gating) was used.

Carotid model geometry reconstruction with the finite element model

The carotid artery geometry was obtained from the multi-sequence MRI data. A custom-made software was used to segment the regions of arterial wall and lumen [15], which have different signal characteristics on multisequence MRI (Figure 1A). After segmentation, the boundary points were imported into the ScanIP computer-modeling and analysis software (ScanIP 3.1, Simpleware Ltd., Exeter, United Kingdom). Each slice was then linked by closed spline interpolation to form complete contours. The regions of interest (ROIs) of each slice corresponding to the plaque contour, wall and lumen, as well as peripheral supporting tissues (to minimize the bending effect caused by pre-axial stretching) surrounding the common carotid artery and the internal and external carotid arteries were delineated (Figure 1B). Contours were reconstructed to form a three-dimensional geometric carotid artery (Figure 1C). To demonstrate the morphology of the vessel, the pink part (peripheral supporting tissue) was removed, because otherwise the vessel would be hidden inside the pink part and become undisplayable. The pink part was used to reduce the deformation of the vessel wall during the calculation process.

The geometry was then imported into the ScanFE computer modeling and analysis software (ScanFE 3.1, Simpleware Ltd., Exeter, United Kingdom) for mesh generation, which subsequently could be exported directly to a finite element solver COMSOL 4.3. Meshing was performed using hexahedron

elements to deal with models including the vascular lumen (yellow), vessel wall including plaque (red) and surrounding tissues (pink), as previously described [20-22].

FSI model and solver

For the fluid model, the blood flow was assumed be an incompressible, homogeneous, Newtonian, viscous fluid with a density of 1050 kg/m³ and a viscosity of 0.0035 Pa·s. The Navier-Stokes equation was used as the governing equation, which was suitable for solutions using FSI modeling and frequent mesh adjustments:

$$\rho_b \frac{\partial v}{\partial t} + \rho_b [(v - v_g) \cdot \nabla] v = -\nabla p + \mu \nabla^2 v$$

where v is the flow velocity, v_g is the mesh velocity, p is the pressure, and μ and ρ_b stand for blood viscosity and density, respectively. A no-slip condition between the fluid and the vessel wall was used, and the inlet boundary condition was specified as the blood-flow velocity at the CCA as measured by MRI-PC. The outlet boundary condition was specified as $P=P_0$, $[\mu(\nabla u + (\nabla u)^T)]n=0$. The plaque, artery wall and peripheral supporting tissue were assumed to be hyper-elastic and to be composed of homogeneous materials. The Neo-Hookean model was used to describe the hyper-elastic material properties of the tissues using the following strain energy function (W):

$$W = \frac{1}{2} \mu (\bar{I}_1 - 3) + \frac{1}{2} K (J - 1)^2$$

where μ is the initial shear modulus, \bar{I}_1 is the first deviatoric strain invariant, J is the ratio of the deformed elastic volume over the undeformed volume, and K is the bulk modulus. The initial bulk modulus K was set to 20 times that of the initial shear modulus. The initial shear modulus μ was set to 6204106 Pa for the vessel wall and 719676 Pa for the peripheral supporting tissue (using COMSOL 4.3). The carotid bloodstream and vessel walls could be stretched axially in the one-way or fully coupled FSI simulations. In the one-way FSI simulation, the fluid model was solved first, and the obtained pressure was transferred to the solid domain as external loading, followed by calculation of the structural stress. No further iteration between the fluid and the solid domains was performed, and non-linear incremental iterative procedures were used to account for the interaction between these two domains in the fully coupled FSI simulation. All models were performed using one-way FSI; additional simulation in 19 models of the diseased group (randomly selected) was conducted using fully coupled FSI. Both types of FSI simulations were performed using COMSOL 4.3 (COMSOL Inc., USA). The maximum von Mises stress, minimum pressure and flow velocity values at the most stenotic location of the patients or at the carotid bifurcation of the healthy volunteers were calculated and assessed using

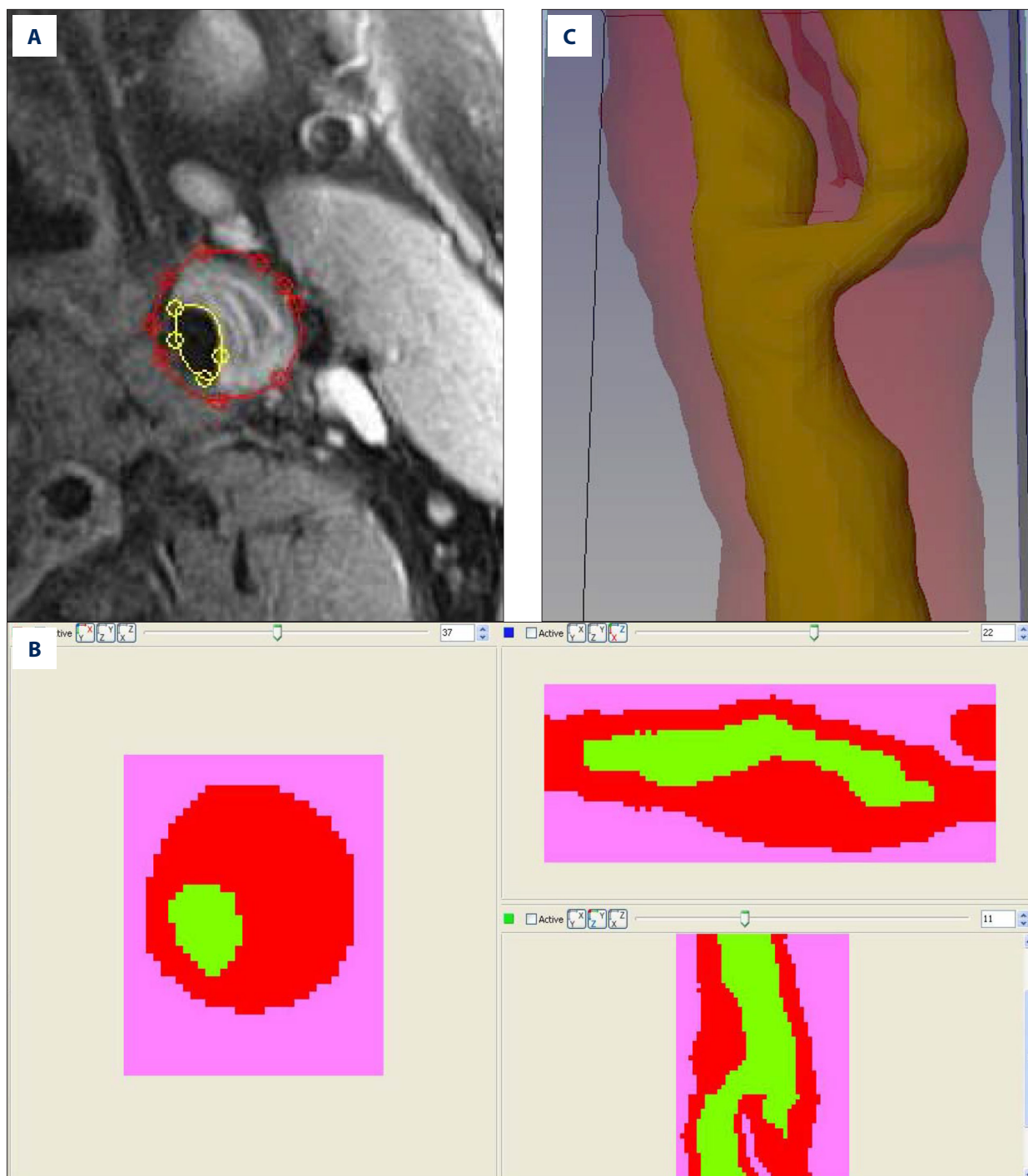
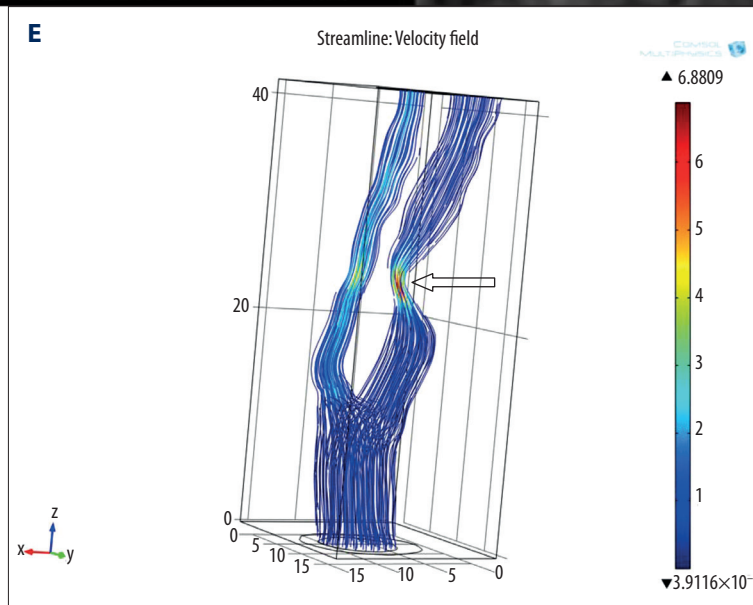
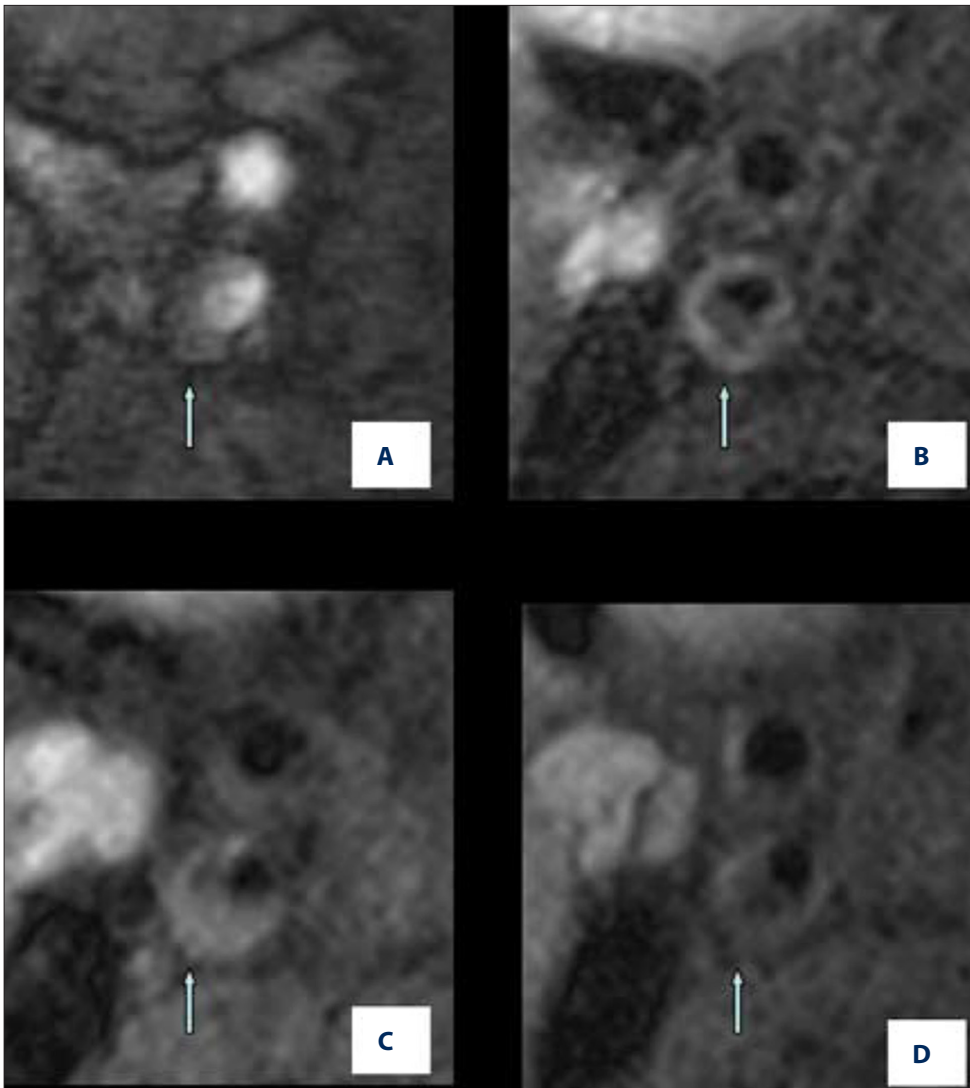


Figure 1. (A) Arterial wall and lumen segmentation. The lumen area in images is darker compared with the arterial wall. The yellow area is the vessel lumen. The area between the yellow and red lines is the vessel wall. (B) The regions of interest (ROIs) were delineated for each slice on the x-y, y-z and x-z planes using the Scan IP software. The different sections are shown using different colors. Yellow: the vascular lumen; red: the vessel wall including plaque; pink: peripheral tissues. (C) Reconstructed three-dimensional geometric carotid artery. Yellow: the vascular lumen; red: vessel wall. To demonstrate the morphology of the vessel, the pink part (peripheral supporting tissues) was removed.



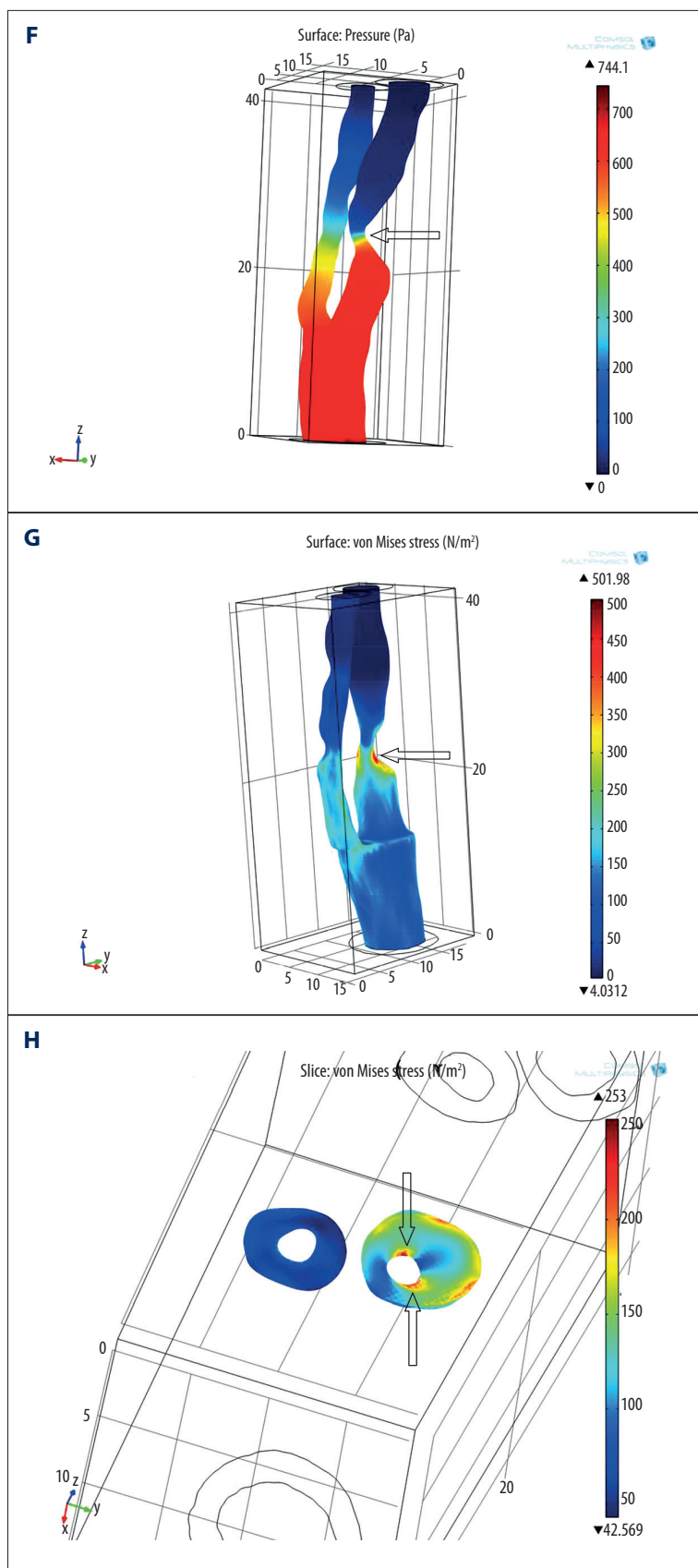
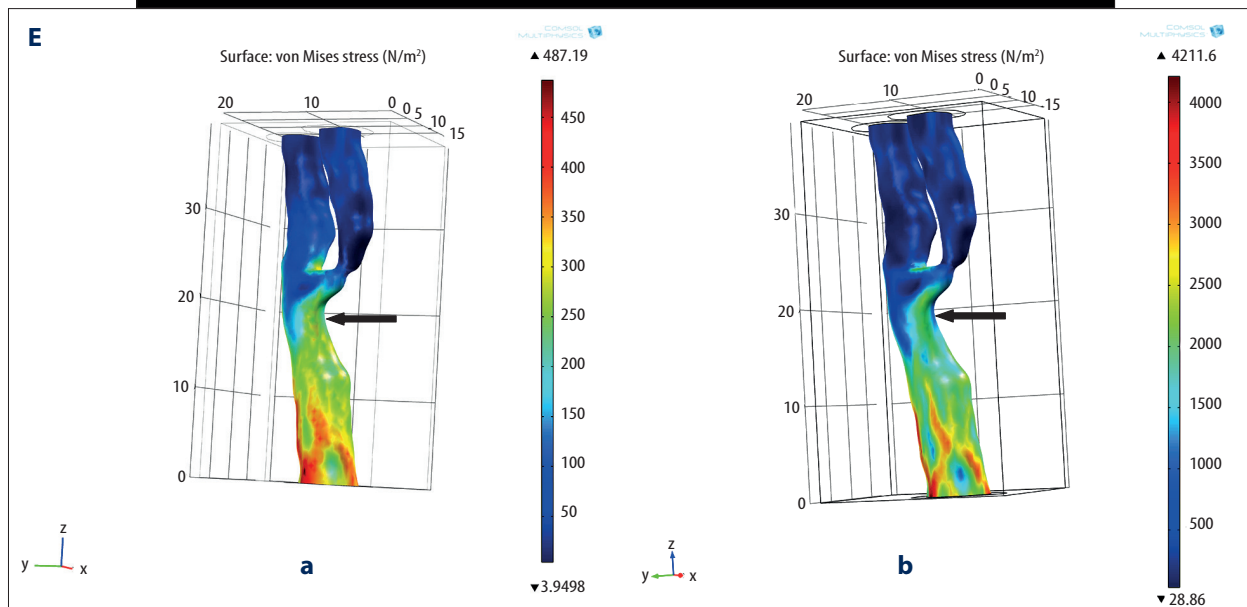
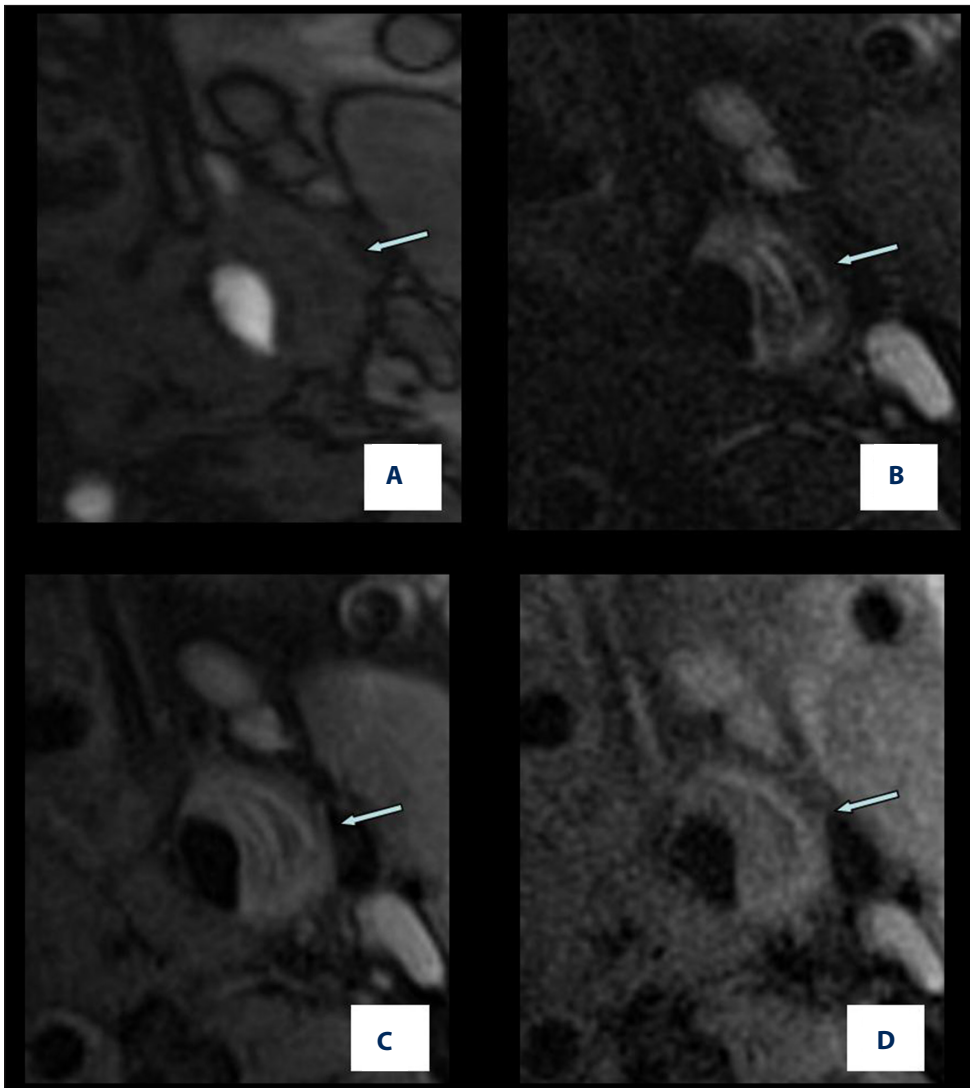


Figure 2. A patient with right internal carotid artery plaque causing stenosis. **(A–D)** MRI image using the TOF, T2WI, PDWI and T1WI protocols, respectively. The arrows indicate the plaques. **(E)** Streamline image showing an increase in flow velocity through the stenosed region (arrow). The color scale varies from red (high velocity) to blue (low velocity). **(F)** Pressure map showing a decrease in pressure at the throat of the plaque (arrow). The color scale varies from red (high pressure) to blue (low pressure). **(G)** von Mises stress maps showing the maximum von Mises stress at the shoulders of the plaque (arrow). The color scale varies from red (high von Mises stress) to blue (low von Mises stress). **(H)** von Mises stress slice maps showing the maximum von Mises stress at the shoulders of the plaque (arrow). The color scale varies from red (high von Mises stress) to blue (low von Mises stress).



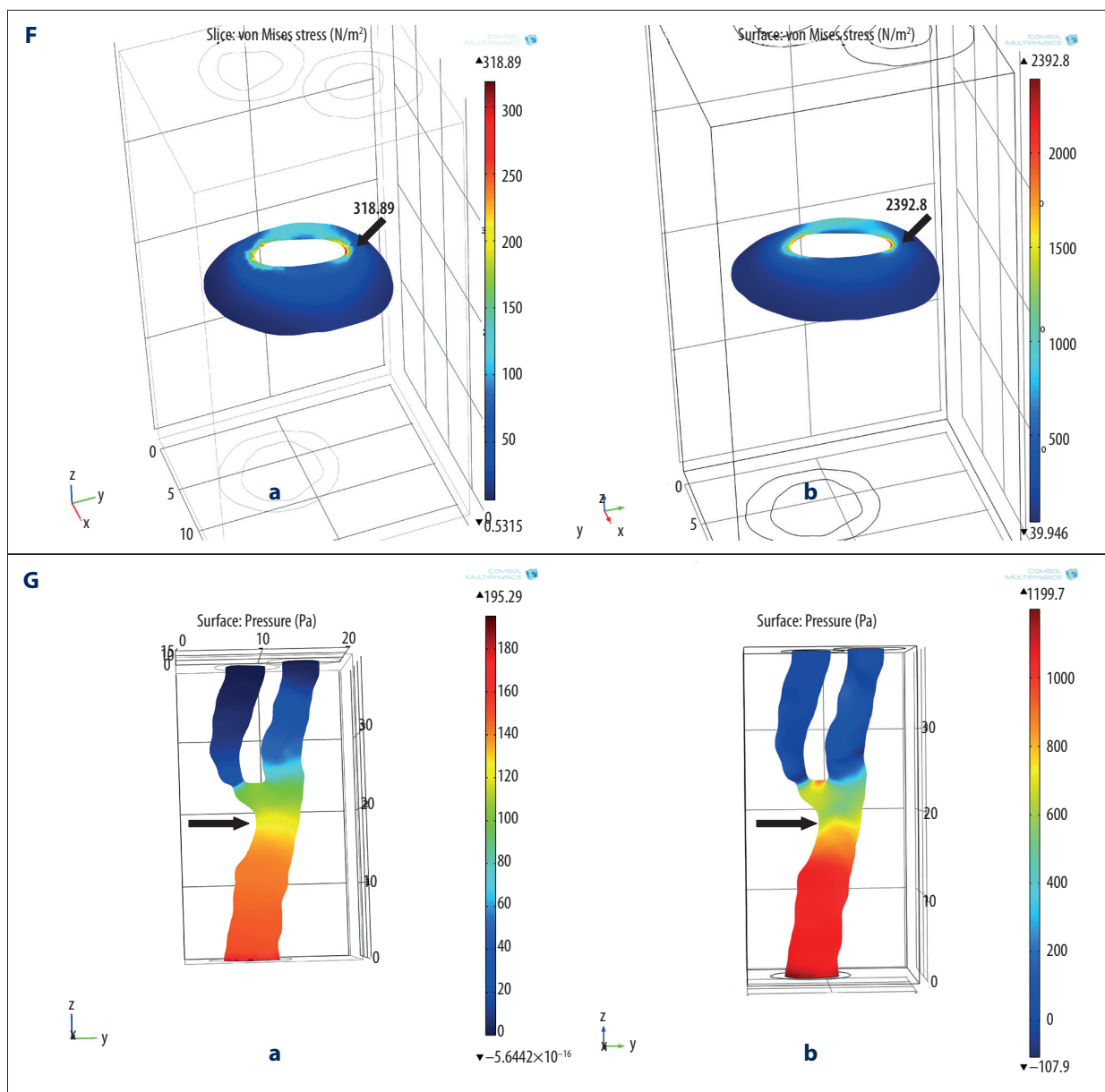


Figure 3. A patient who underwent both one-way FSI and fully coupled FSI. MRI shows a plaque in the left common carotid artery. (A–D) MRI using the TOF, T2WI, PDWI and T1WI protocols, respectively. The arrows indicated the plaques. (E) Comparison of the von Mises stress of the one-way FSI (a) and fully coupled FSI (b). The map of the one-way FSI shows an increase in stress near the plaques (black arrow). The von Mises stress map of the fully coupled FSI shows that stress is elevated near the plaque (black arrow). Although there were differences in the numerical values of the von Mises stress in the two simulation types, their tendencies and distributions were identical. The color scale varies from red (high von Mises stress) to blue (low von Mises stress). (F) Comparison of cross-sectional slices of the von Mises stress of the one-way FSI (a) and fully coupled FSI (b). Both show that the maximum von Mises stress is at the shoulders of the plaque (black arrow), but the numerical values are different. The numerical values of fully coupled FSI were high. (G) Comparison of plaque pressure of the one-way FSI (a) and fully coupled FSI (b). The pressure map of the one-way FSI shows a reduction in pressure at the throat of the plaque (black arrow). The pressure map of the fully coupled FSI shows a drop in pressure at the throat of the plaque (black arrow). Although there were differences in the numerical values of pressure between the two simulation types, their tendencies and distributions were identical. The color scale varies from red (high pressure) to blue (low pressure).

Table 1. Hemodynamic parameters between the carotid artery stenosis and the control groups.

Parameter	Healthy participants	Patients with carotid plaques	P-value
Maximum von Mises stress (N/m ²)	35.45 (29.24)	200.99 (326.99)	<0.001
Minimum pressure (Pa)	11.30 (11.11)	69.71 (99.39)	<0.001
Velocity (m/s)	0.65±0.23	2.76±1.81	<0.001

Data are presented as median and interquartile range (von Mises and minimum pressure) or mean ± standard deviation (velocity).

one-way FSI. For 19 models from the patients, values for both fully coupled and one-way FSI simulations were calculated and compared.

Statistical analysis

The maximum von Mises stress, minimum pressure and flow velocity values are presented as mean ± standard deviation (SD) or median and interquartile range (IQR). The normality of the data was assessed using the one-sample Kolmogorov-Smirnov test. The statistical analysis was performed using SPSS 19.0 (IBM, Armonk, NY, USA). All tests were two-tailed, and P-values <0.05 were considered to be statistically significant.

Comparison of hemodynamic parameters based on one-way FSI

The maximum von Mises stress and minimum pressure values were compared between the control and carotid plaque groups using the Mann-Whitney U test. The independent samples t-test was used to determine the statistical significance of any differences in the velocity between the control and carotid plaque groups. The independent samples t-test was used for normally distributed data, and the Mann-Whitney U test was used for non-normally distributed data.

Differences between fully coupled FSI and one-way FSI in 19 patients

The maximum von Mises stress and velocity values were compared between the one-way FSI group and the fully coupled FSI group using a paired samples t-test. The Wilcoxon test was used to determine the statistical significance of any differences in the minimum pressure between the one-way FSI and fully coupled FSI groups. The paired samples t-test was used for normally distributed data, and the Wilcoxon test was used for non-normally distributed data.

Differences of the maximum von Mises stress between diseased subgroups

The maximum von Mises stress was compared between the stable plaque group and the vulnerable plaque group using

the Mann-Whitney U test because of non-normally distributed data. The maximum von Mises stress was compared between the groups with and without fibrous cap defects using the independent samples t-test because of normally distributed data.

Results

Characteristics of the participants

Patients with carotid artery atherosclerosis were aged 57.6±12.5 years and included 45 males and 7 females. The healthy participants without carotid artery atherosclerosis were aged 50.6±12.9 years and included 11 males and one female.

Hemodynamic parameters based on one-way FSI

The models of 86 carotid artery plaques (Figure 2A–2D and Figure 3A–3D) and 14 normal carotid bifurcations were assessed. The flow velocity accelerated as blood passed through the region of stenosis, leading to a decline in pressure. Areas with maximum velocity and minimum pressure were located at the throat of the plaques (Figure 2E, 2F). The maximum von Mises stress in the plaques was detected at the top of the plaque or at the shoulders of the plaques, but those at the shoulders were more frequent (Figure 2G, 2H).

Significant differences were detected in the maximum von Mises stress, minimum pressure and blood velocity between the CAD and control groups (all P<0.05) (Table 1).

Difference between one-way FSI and fully coupled FSI

Maximum velocity and minimum pressure were observed at the throat of the plaques using both one-way FSI and fully coupled FSI (Figure 3). The maximum von Mises stress in the plaques was located at the top of the plaque or at the shoulders of the plaques using both one-way FSI and fully coupled FSI (Figure 3E, 3F).

The maximum von Mises stress and the minimum pressure were significantly higher and the velocity was significantly lower based on fully coupled FSI compared with one-way FSI

Table 2. Hemodynamic parameters in the one-way FSI group and the fully coupled FSI group (n=19).

Parameter	Fully coupled FSI group	One-way FSI group	P-value
Maximum von Mises stress (N/m ²)	4532.68±4643.92	531.17±462.79	0.001
Minimum pressure (Pa)	651.30 (2329.50)	112.63 (316.04)	<0.001
Velocity (m/s)	1.55±0.84	1.95±0.87	<0.001

Data are presented as median and interquartile range (minimum pressure) or mean ± standard deviation (Maximum von Mises stress and velocity).

(all $P < 0.05$). Compared with fully coupled FSI, one-way FSI underestimated the stress and minimum pressure and overestimated the velocity (Table 2).

Although there were differences in the numerical values of the hemodynamic parameters between fully coupled and one-way FSI simulation, their tendencies and distributions were identical (Figure 3E–3G).

Maximum von Mises stress of plaques

There were 86 cases of carotid atherosclerotic plaques, of which the plaques were stable in 47 cases, and vulnerable in 39. Among the 39 vulnerable plaques, 16 had fibrous cap defects and 23 were without defect. According to one-way FSI, the maximum von Mises stress of the stable and vulnerable plaques were 113.08 (127.434) N/m² (median and IQR) and 414.13 (718.19) N/m² (median and IQR), respectively ($P < 0.001$).

The maximum von Mises stress of the group with fibrous cap defect and that of the group without defect were 1194.43±841.93 N/m² (mean ±SD) and 305.80±207.83 N/m² (mean ±SD), respectively ($P = 0.001$).

Discussion

The aim of the present study was to develop a system to assess the hemodynamics of carotid atherosclerotic plaques using subject-specific FSI models based on MRI. Results showed that the maximum von Mises stress and the minimum pressure and velocity were significantly increased in the stenosis group compared with controls based on one-way FSI. The maximum von Mises stress and the minimum pressure were significantly higher and the velocity was significantly lower based on fully coupled FSI compared with one-way FSI. Although there were differences in numerical values, both methods were equivalent. The maximum von Mises stress of vulnerable plaques was significantly higher than stable plaques. The maximum von Mises stress of the group with fibrous cap defect was significantly higher than that of the group without defect. These results are supported by previous findings [23,24]. Indeed, high

stress levels acting on the endothelium are reported to have a regressive effect on underlying intimal tissue, leading to destabilization of plaque [25,26]. We found that the maximum von Mises stress of vulnerable plaques was higher than that of the stable plaques, while the maximum von Mises stress of the group with fibrous cap defect was significantly higher than that of the group without defect.

Geometric reconstruction

The accuracy of the FSI simulation depends on an accurate geometrical reconstruction of the plaque and vessel geometry. To approximate the physiological conditions, we used 3D geometric and morphologic data derived from *in vivo* MRIs of patients and healthy volunteers to reconstruct the plaque and vessel geometries of the carotid bifurcation. This study design is different from that of previous studies on FSI, which derived the geometry from MRI or *ex vivo* MR imaging [15]. Indeed, any change in the shape of the vessels and plaques as a result of endarterectomy and histologic fixation would significantly affect the biomechanical parameter distributions [27,28]. There are a number of problems associated with deriving plaque and blood vessel geometry from histological data. First, endarterectomy specimens do not include the entire thickness of the artery, and the process of harvesting the plaque frequently involves entry into the lumen, thereby altering its morphology. Second, histological processing, including decalcification and fixation, could significantly alter the plaque morphology and cause shrinkage of the specimen. Finally, a fixed specimen lacks pressure within the lumen, which would maintain its shape [29]. Therefore, the major advantages of determining the vessel geometry of plaque from *in vivo* MRI is that the luminal morphology can be most effectively determined under physiological conditions in which the blood pressure maintains the lumen shape.

FSI simulation

In our FSI model, the artery wall, plaque and peripheral supporting tissue were assumed to be composed of hyper-elastic material that could stretch and expand to approximate the physiological conditions. The Neo-Hookean model was used to

specify the hyper-elastic material properties. This model has been considered to be valid for the moderate deformations that occur in atherosclerotic plaques and was validated to produce geometry similar to that of a previously described model [13,30]. Additionally, the modified Mooney-Rivlin [12,14,15] and Ogden hyper-elastic models [31,32] have been used. Because various hyper-elastic models and material specifications might substantially affect the hemodynamic parameters, any comparison of the parameters based on different models should be interpreted with caution. In the present study, the stress level was calculated using von Mises stress, whereas other investigators have used first-principal stresses [13,16,23]. The von Mises criterion is a formula that combines three stresses into one equivalent stress, which is compared to the yield stress of the material, and it calculates whether the combined stress at a given point would lead to collapse. The rupture of a vulnerable plaque occurs as a result of failure of structure when the local internal stress is greater than the strength limit of the fibrous cap. Thus, von Mises stress should be better suited for stress analyses compared with other stress estimates. A study has shown that there was not much difference between using Stress-P1 and von Mises to describe the stress level at vulnerable sites [33].

Hemodynamic parameters

Results showed that the flow velocity increased when passing through a region of stenosis, and the maximum velocity was located at the throat of the plaque, which is in agreement with previous studies [24,34]. According to the Bernoulli principle, increased blood velocity across the lumen reduces the lateral blood pressure acting on the plaque. We observed minimum pressure at the throat of the plaques, which was consistent with previous findings [15,35], and the minimum pressure near the plaque was higher in the plaque group. Li et al. [35] have suggested that although the local high stress at the stenosis region might damage the endothelium and cause plaque rupture, the magnitude of stress was small compared with the overall load on the plaque. The effect of pressure should be considered in an analysis of plaque stability and of the mechanical causes of plaque rupture.

Comparison of the fully coupled FSI and one-way FSI simulations

To compare differences in hemodynamic parameters between the fully coupled and one-way FSI models, an additional fully coupled FSI simulation was carried out in 19 randomly selected plaque models. The results showed that the maximum von Mises stress and minimum pressure were higher and the velocity was lower based on the fully coupled FSI compared with one-way FSI. Indeed, one-way FSI does not feed

information on arterial wall deformation back into the blood flow calculations, resulting in a loss of accuracy when determining hemodynamic parameters such as stress and pressure. Therefore, a fully coupled FSI simulation should provide more precise data than a one-way FSI simulation regarding predicted blood flow, stress and pressure distributions in the plaque region. To put it another way, the one-way FSI model underestimate stress and pressure and overestimate velocity compared with the fully coupled FSI model. The numerical accuracy and reliability of the fully coupled FSI analyses have been previously demonstrated and validated [36]. Although there were differences in the numerical values of these hemodynamic parameters in the two simulation types, their tendencies and distributions were identical. Fully coupled FSI is more accurate, but it requires much greater computational resources. The time taken for a fully coupled FSI simulation for each single carotid model was 5 days on mean (range 3–7 days), whereas the simulation time for one-way FSI of the identical model was only 5–10 minutes using the same computer. Therefore, one-way FSI resulted in a reasonably accurate estimation with significantly less computational effort compared with the fully coupled FSI approach; it should be a good compromise that provides more realistic loading conditions for hemodynamic analysis.

The present study also had some limitations. First, there was no histology of the plaques in the study because the carotid endarterectomy procedure is not a routine procedure in our hospital and because the MRI was performed *in vivo*. However, previous studies have shown that there is a high level of agreement between MRI and histology of the plaques [17–19]. Second, cases with fully coupled FSI were limited because it requires much greater computational resources and too much time. Indeed, the time taken for a fully coupled FSI simulation for each single carotid model was 5 days on mean (range 3–7 days), whereas the simulation time for one-way FSI of the identical model was only 5–10 minutes using the same computer. Further study is necessary to fully compare the two approaches.

Conclusions

To the best of our knowledge, this study is the first to demonstrate the effectiveness of a platform for evaluating plaque hemodynamic based on FSI using *in vivo* high-resolution MRI on a relatively large patient sample. In conclusion, the hemodynamics of atherosclerotic plaques can be assessed noninvasively using subject-specific models of FSI based on MRI. Especially, one-way FSI is more suitable for clinical application. These data can be used to stratify patients at risk of carotid atheroma and provide a noninvasive method for patient monitoring.

Acknowledgments

The authors thank the participants for their invaluable contribution. The authors acknowledge the work of the staff at the Radiology Department.

References:

- Brott TG, Halperin JL, Abbara S et al: 2011 ASA/ACCF/AHA/AANN/AANS/ACR/ASNR/CNS/SAIP/SCAI/SIR/SNIS/SVM/SVS guideline on the management of patients with extracranial carotid and vertebral artery disease: executive summary. *Stroke*, 2011; 42(8): e420–63
- Grotta JC: Clinical practice. Carotid stenosis. *N Engl J Med*, 2013; 369(12): 1143–50
- Thapar A, Jenkins IH, Mehta A, Davies AH: Diagnosis and management of carotid atherosclerosis. *BMJ*, 2013; 346: f1485
- Roger VL, Go AS, Lloyd-Jones DM et al: Heart disease and stroke statistics – 2011 update: a report from the American Heart Association. *Circulation*, 2011; 123(4): e18–e209
- Petty GW, Brown RD Jr, Whisnant JP et al: Ischemic stroke subtypes: a population-based study of functional outcome, survival, and recurrence. *Stroke*, 2000; 31(5): 1062–68
- Fuster V, Moreno PR, Fayad ZA et al: Atherothrombosis and high-risk plaque: part I: evolving concepts. *J Am Coll Cardiol*, 2005; 46(6): 937–54
- Taussky P, Hanel RA, Meyer FB: Clinical considerations in the management of asymptomatic carotid artery stenosis. *Neurosurg Focus*, 2011; 31(6): E7
- Rundek T, Arif H, Boden-Albala B et al: Carotid plaque, a subclinical precursor of vascular events: the Northern Manhattan Study. *Neurology*, 2008; 70(14): 1200–7
- Lovett JK, Rothwell PM: Site of carotid plaque ulceration in relation to direction of blood flow: an angiographic and pathological study. *Cerebrovasc Dis*, 2003; 16(4): 369–75
- Malek AM, Alper SL, Izumo S: Hemodynamic shear stress and its role in atherosclerosis. *Jama*, 1999; 282(21): 2035–42
- Nerem RM: Vascular fluid mechanics, the arterial wall, and atherosclerosis. *J Biomech Eng*, 1992; 114(3): 274–82
- Huang Y, Teng Z, Sadat U et al: The influence of computational strategy on prediction of mechanical stress in carotid atherosclerotic plaques: comparison of 2D structure-only, 3D structure-only, one-way and fully coupled fluid-structure interaction analyses. *J Biomech*, 2014; 47(6): 1465–71
- Kock SA, Nygaard JV, Eldrup N et al: Mechanical stresses in carotid plaques using MRI-based fluid-structure interaction models. *J Biomech*, 2008; 41(8): 1651–58
- Tang D, Yang C, Canton G et al: Correlations between carotid plaque progression and mechanical stresses change sign over time: a patient follow up study using MRI and 3D FSI models. *Biomed Eng Online*, 2013; 12: 105
- Tang D, Yang C, Zheng J et al: 3D MRI-based multicomponent FSI models for atherosclerotic plaques. *Ann Biomed Eng*, 2004; 32(7): 947–60
- Zheng J, Abendschein DR, Okamoto RJ et al: MRI-based biomechanical imaging: initial study on early plaque progression and vessel remodeling. *Magn Reson Imaging*, 2009; 27(10): 1309–18
- Saam T, Ferguson MS, Yarnykh VL et al: Quantitative evaluation of carotid plaque composition by *in vivo* MRI. *Arterioscler Thromb Vasc Biol*, 2005; 25(1): 234–39
- Chu B, Kampschulte A, Ferguson MS et al: Hemorrhage in the atherosclerotic carotid plaque: a high-resolution MRI study. *Stroke*, 2004; 35(5): 1079–84
- Cai JM, Hatsukami TS, Ferguson MS et al: Classification of human carotid atherosclerotic lesions with *in vivo* multicontrast magnetic resonance imaging. *Circulation*, 2002; 106(11): 1368–73
- Wu Z, Yang C, Tang D: *In vivo* serial MRI-based models and statistical methods to quantify sensitivity and specificity of mechanical predictors for carotid plaque rupture: location and beyond. *J Biomech Eng*, 2011; 133(6): 064503
- Huang X, Teng Z, Canton G et al: Intraplaque hemorrhage is associated with higher structural stresses in human atherosclerotic plaques: an *in vivo* MRI-based 3D fluid-structure interaction study. *Biomed Eng Online*, 2010; 9: 86
- Huang X, Yang C, Canton G et al: Quantifying effect of intraplaque hemorrhage on critical plaque wall stress in human atherosclerotic plaques using three-dimensional fluid-structure interaction models. *J Biomech Eng*, 2012; 134(12): 121004
- Tang D, Teng Z, Canton G et al: Sites of rupture in human atherosclerotic carotid plaques are associated with high structural stresses: an *in vivo* MRI-based 3D fluid-structure interaction study. *Stroke*, 2009; 40(10): 3258–63
- Jing LN, Gao PY, Lin Y et al: Distribution of wall shear stress in carotid plaques using magnetic resonance imaging and computational fluid dynamics analysis: a preliminary study. *Chin Med J*, 2011; 124(10): 1465–69
- Kenagy RD, Fischer JW, Davies MG et al: Increased plasmin and serine proteinase activity during flow-induced intimal atrophy in baboon PTFE grafts. *Arterioscler Thromb Vasc Biol*, 2002; 22(3): 400–4
- Cucina A, Sterpetti AV, Borrelli V et al: Shear stress induces transforming growth factor-beta 1 release by arterial endothelial cells. *Surgery*, 1998; 123(2): 212–17
- Lee RT: Atherosclerotic lesion mechanics versus biology. *Z Kardiol*, 2000; 89(Suppl.2): 80–84
- Loree HM, Kamm RD, Stringfellow RG, Lee RT: Effects of fibrous cap thickness on peak circumferential stress in model atherosclerotic vessels. *Circ Res*, 1992; 71(4): 850–58
- Li ZY, Howarth S, Trivedi RA et al: Stress analysis of carotid plaque rupture based on *in vivo* high resolution MRI. *J Biomech*, 2006; 39(14): 2611–22
- Li ZY, Howarth SP, Tang T, Gillard JH: How critical is fibrous cap thickness to carotid plaque stability? A flow-plaque interaction model. *Stroke*, 2006; 37(5): 1195–99
- Li ZY, Howarth SP, Tang T et al: Structural analysis and magnetic resonance imaging predict plaque vulnerability: a study comparing symptomatic and asymptomatic individuals. *J Vasc Surg*, 2007; 45(4): 768–75
- Versluis A, Bank AJ, Douglas WH: Fatigue and plaque rupture in myocardial infarction. *J Biomech*, 2006; 39(2): 339–47
- Sadat U, Teng Z, Gillard JH: Biomechanical structural stresses of atherosclerotic plaques. *Expert Rev Cardiovasc Ther*, 2010; 8(10): 1469–81
- Li ZY, Tan FP, Soloperto G et al: Flow pattern analysis in a highly stenotic patient-specific carotid bifurcation model using a turbulence model. *Comput Methods Biomech Biomed Eng*, 2015; 18(10): 1099–107
- Li ZY, Taviani V, Tang T et al: The mechanical triggers of plaque rupture: shear stress vs. pressure gradient. *Br J Radiol*, 2009; 82(Spec No 1): S39–45
- Tang D, Yang C, Kobayashi S et al: Effect of stenosis asymmetry on blood flow and artery compression: a three-dimensional fluid-structure interaction model. *Ann Biomed Eng*, 2003; 31(10): 1182–93

Competing interests

All authors declare that they have no conflict of interest.